SYNTHESIS OF CARBON NANOTUBES/SNO_2 CORE-SHELL NANOWIRES AND THEIR GAS SENSITIVITY TO ALCOHOL

Xiaohan DU[1], Dongfang GUO[2], Yanyue LIU[2], Zijiong LI[2*]

In this paper, we report the synthesis of CNTs/SnO_2 core-shell composite materials by a novel method. It shows that the SnO_2 nucleation and growth on the outer wall of CNTs result in the formation of core-shell structure nanowires with uniform layer of parcels. We tested the gas sensitivity of the CNTs/SnO_2 composites to ethyl alcohol by static method, and found that the introduction of CNTs in the SnO_2 composite materials results in a decrease in their optimum operating voltage, with the optimum at V_H = 3.5 V, and an increase in their gas sensitivity. We also found that as the operating voltage increases, the gas sensing of the CNTs/SnO_2 composites decreases after at first increasing with the alcohol concentration increases. The sensitivity of the composites to alcohol gradually increases and tends to reach a constant finally. Moreover, the sensitivity reaches the maximum at concentration level of 800 ppm ethyl alcohol.

Keywords: Carbon nanotubes, SnO_2, Composites, Gas sensitivity

1. Introduction

Carbon nanotubes (CNTs) have a unique quasi-one-dimensional nanostructure with good conductivity and chemical stability. The composite nanostructures produced by deposition of functional metal oxide nanoparticles on the surface of CNTs can prevent the agglomeration of the CNTs which can improve surface conductivity when compared with pure CNTs [1-8]. Much has been done in recent years in the researches on the carbon nanotubes coated various functional metal oxide nanoparticles. The multiple functions of SnO_2, in particular, have made CNTs/SnO_2 composites a subject of extensive researches, especially their gas sensitivity [9-14].

In recent years, researchers have paid great attention to the gas sensitive to alcohol. Various kinds of SnO_2 and its composites have been used to gas sensors. However, how to produce novel structure of SnO_2 and composites with excellent in alcohol sensitivity is still the focus of attention in this area.

In this paper, the CNTs/ SnO_2 core-shell nanowires were synthesized, and their structures were also analyzed as well as the process of their formation. We

[1] School of Physics and Electronics, North China University of Water Resources and Electric Power, Zhengzhou, China; E-mail: duxiaohan@ncwu.edu.cn

2 School of Physics and Electronics, Zhengzhou University of Light Industry, Zhengzhou, China; E-mail: zijiongli@zzuli.edu.cn

also tested their gas sensitivity so as to study the influence of the structure of the CNTs/ SnO_2 nano composites on their gas sensitivity.

2. Experimental

2.1 The synthesis of CNTs/SnO_2 nanocomposites

CNTs with 25-40 nm in diameter and the solution of $SnCl_2$ were used to produce the CNTs /SnO_2 composites. First the CNTs were treated with the reflux method in HNO_3 solution (with the percentage of solution by mass at 40%) at 100 ℃ for 2 hours, so that the oxygen-containing functional groups can be formed on the surface of the CNTs, which help the hydrophily of the CNTs in the solution. Then we used ultrasound dispersion of 100 mg the HNO_3-treated CNTs in 400 mL of deionized water and added to them 1.3 mL of HCl solution (38%) and 10 g of $SnCl_2 \cdot 2H_2O$ to it and stirred the solution for them to react for 2 hours. We got CNTs/SnO_2 after the processes of filtration, washing with deionized water and allowing the materials to dry in the air at 90 ℃ for 6 hours.

The morphology and structure of the nanocomposites were examined by FESEM (HITACH IS4 700) and TEM (JEOL 2010. X-ray diffraction (XRD) was applied on Bruker D8 Advance instrument with Cu Kα radiation. The Raman spectrum was measured on LabRAM HR800 with an excitation laser wavelength of λ = 532 nm. Thermogravimetric analysis (TGA) was carried out on an SDT Q600 (TA) instrument under air flow (10 °C min-1) up to 700 °C.

2.2 Gas sensitivity tests

We use the static method to test the gas sensitivity of the nanostructure composites, and the electrical circuit is shown in Fig. 1. Changes in the voltage on the nodes of the resistor correlate with the resistance of the gas sensitive materials in the air and the gas used for the tests. The test of SnO_2 will be based on V_C =10 V, while the tests on CNTs /SnO_2 will be based on V_C=5 V.

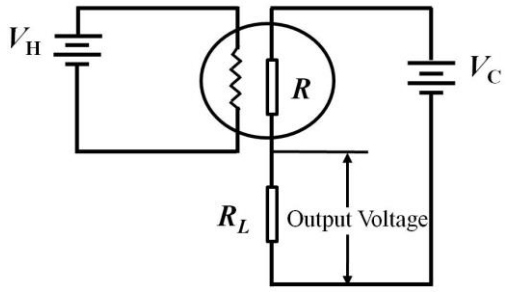

Fig.1 Circuit for gas sensitivity testing.

In the Fig. 1, R is the resistor with a resistance of 5 kΩ, V_H is the supply voltage used for heating; V is the output voltage.

We measure the gas sensitivity β by the following definition,

$$\beta = R_o/R_g \quad (1)$$

R_o is the electrical resistance of the gas sensor in the air, while R_g is the resistance of the gas sensor in the gas used in the tests.

3. Results and discussion

Fig. 2 presents the SEM images of CNTs / SnO_2 nanostructures. As can be seen, the SnO_2 grains are evenly distributed to form a layer of parcel on the outer wall of the CNTs, creating core-shell structure nanowires. Fig. 3 is the TEM image of CNTs /SnO_2 nanostructures, which shows the external wall of the CNT is coated with a 6-10 nm thin layer of SnO_2.

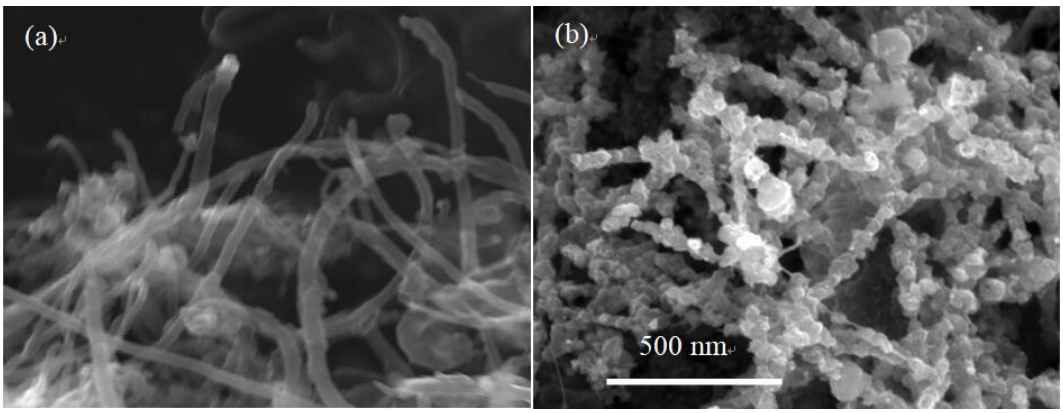

Fig. 2 SEM images of (a) CNTs; (b) CNTs/SnO_2

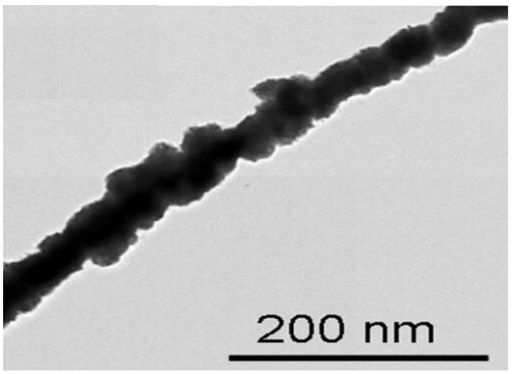

Fig. 3 TEM image of CNTs /SnO_2 nanostructure

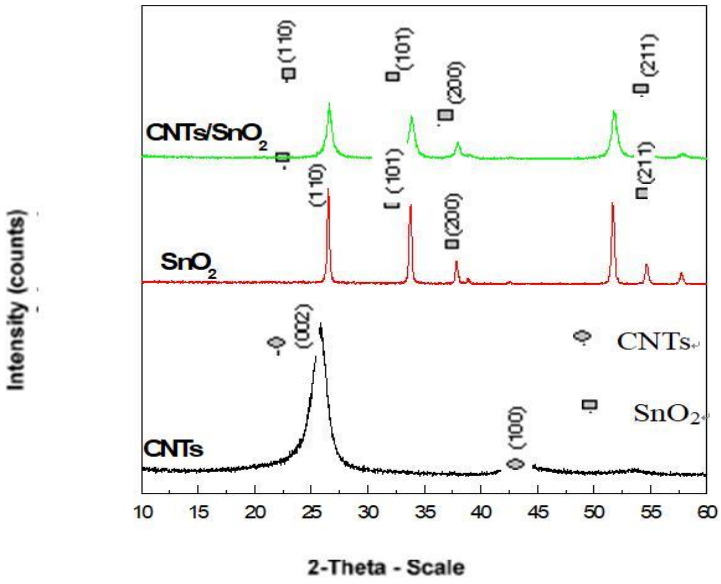

Fig. 4 X-ray diffraction patterns of CNTs, SnO_2 and CNTs /SnO_2

Fig. 4 is the result of the X-ray diffraction tests for CNTs, SnO_2 and CNTs /SnO_2, respectively. As we can see, there are prominent peaks at about 26° for the CNTs and at about 43.5°, which correspond with the diffraction of the graphite plans (002) and (100) of the crystal face when we compare them with a standard (JCPDS 41-1487). The peak in the pattern of SnO_2 in the CNTs /SnO_2 composite roughly coincides with the intensity peak of pure SnO_2, but there is a difference – the peak for SnO_2 in the CNTs /SnO_2 composite is broadened, showing the SnO_2 grains are smaller.

We can also see from the Fig. 4 that the value of the intensity peak for the SnO_2 becomes weaker with the introduction of the CNTs, which can be explained by the lower mass percent composition of the SnO_2 in the sample nanocomposites, when compared with pure SnO_2.

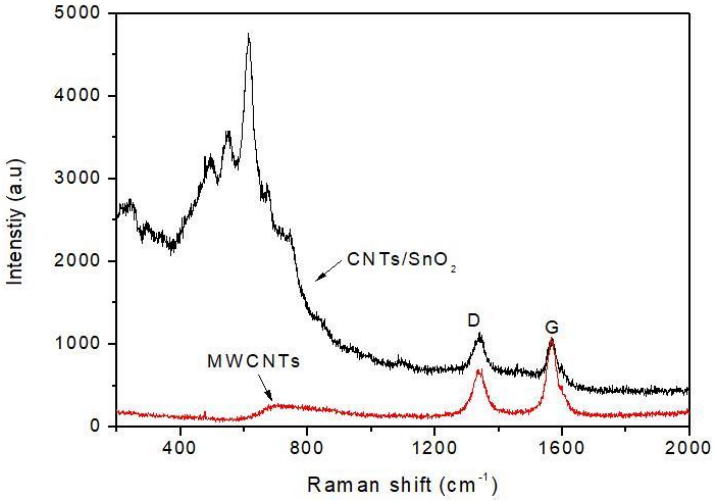

Fig. 5 Raman spectra of CNTs and CNTs/SnO_2

Fig. 5 shows the Raman spectra of the CNTs and the CNTs /SnO_2. As we can see, peaks in intensity for CNTs/SnO_2 are still observed at 1342 cm^{-1} and 1567.6 cm^{-1}, which correspond with CNTs' D peak (D band) and G peak (G band), respectively. The D peak intensity of CNTs/SnO_2 is significantly stronger compared with that of CNTs, reflecting increased disorder. This can be explained by the treatment of CNTs in the process of synthesizing CNTs/SnO_2, which serves a function close to cutting them and thereby increases the defects in the CNTs.

We can also observe some peaks of high energy intensity at the lower section of the spectra for CNTs/SnO_2. This can be explained by the introduction of SnO_2.

Based on these analyses, we think that the SnO_2 coating on the CNTs is formed through a mechanism like this: first, the reflux treatment of the purified CNTs in HNO_3 solution serves a function close to cutting the nanostructures, creating many defects; while at the same time, the oxygen-containing functional groups are formed on the surface of the CNTs, helping the CNTs diffusion in the solution; in addition, the ultrasound dispersing process helps the CNTs to dissolve in the deionized water, too, to create a balanced solution. When we add $SnCl_2 \cdot 2H_2O$ to the solution and stir it, the Sn^{2+} reacts with the O_2,

$$2\ Sn^{2+}+O_2+2\ H_2O=2\ SnO_2+4\ H^+ \qquad (2)$$

Given the large amount of functional groups and defects on the surfaces of the CNTs, the Sn^{2+} contained particles are adsorbed to the surface of the CNTs to

form nuclei and create layers of SnO_2. Here we have the CNTs/SnO_2 nanowires with core-shell structures.

A TG analysis on the CNTs/SnO_2 composite materials was also tested. As shown in Fig. 6, there is a weight loss step at about 600 ℃, with the weight of the sample decreasing by about 10%. The carbon nanotubes start to be oxygenated at about 600 ℃, leading to the weight loss. Therefore, the CNTs account for about 10% of the CNTs /SnO_2 composites in terms of mass percentage.

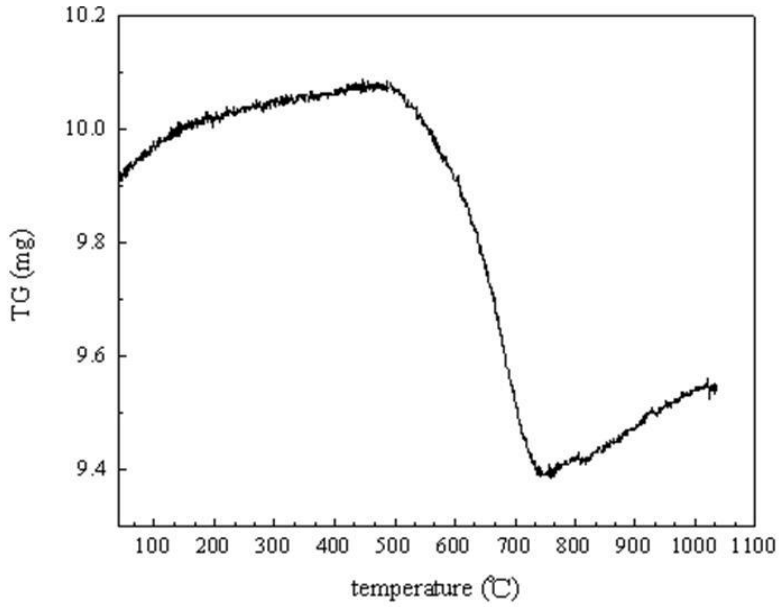

Fig. 6. TGA analysis of CNTs /SnO_2

Fig. 7 shows the results of the gas sensitivity tests. As we can see from Fig. 7a, the optimal working voltage for SnO_2 is at V_h=4.0 V, whereas the optimal working voltage for CNTs/SnO_2 composites is V_h=3.5 V. This value is higher than the similar ones from literature. The reason may be that the introduction of CNTs leads to a decrease in the optimal working temperature. The SnO_2 gas sensor works better at room temperature when compared with CNTs/SnO_2.

As shown in Fig. 7b, the electrical resistance of SnO_2 gradually decreases as the temperature is higher, which can be explained by the desorption of the adsorbed oxygen as the temperature rises, leading to a decrease in the electron barrier and hence a decrease in the electrical resistance of the SnO_2 device. At room temperature, the electrical resistance of CNTs/SnO_2 device is weaker than that of pure SnO_2.

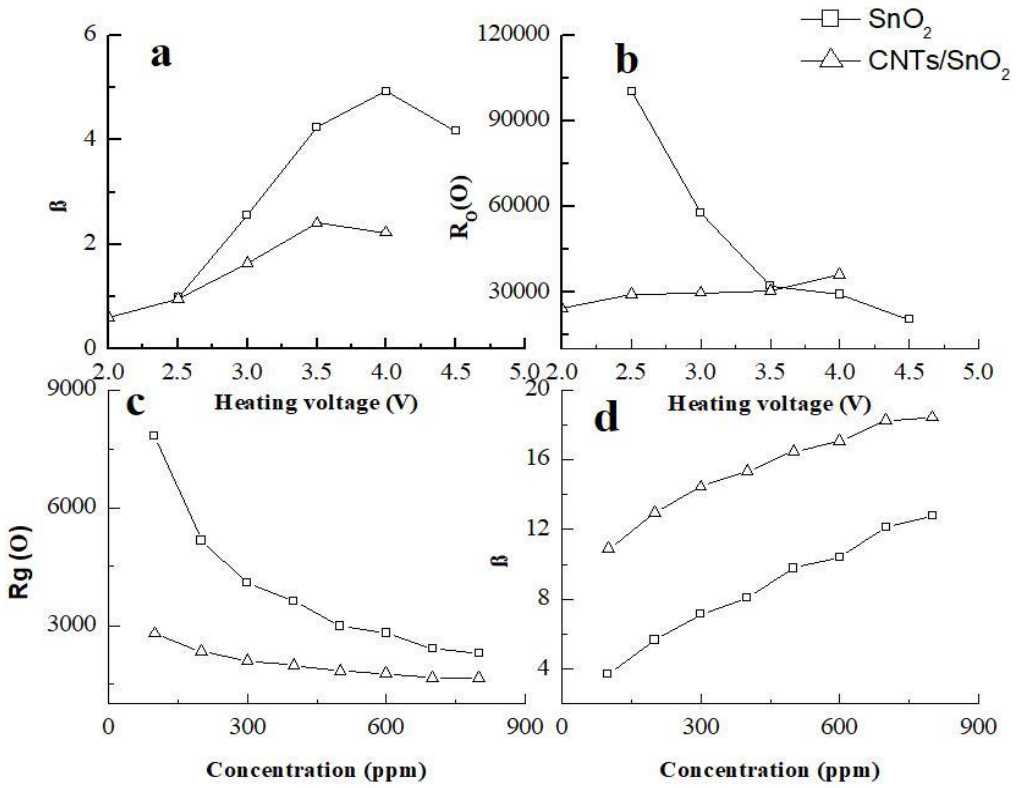

Fig. 7 Gas sensitivity for ethyl alcohol of SnO_2 and CNTs/SnO_2. a) Changes in gas sensitivity in the air as heating voltage increases; b) Changes in electrical resistance as heating voltage increases; c) Changes in electrical resistance as concentration of alcohol increases; d) Changes in gas sensitivity as concentration of alcohol increases.

The reason can be explained tht the metallic nanotubes in the CNTs have good conductivity. However, as the temperature raises further, the electrical resistance of the composite materials increases, this is because the lattice vibration of the CNTs is aggravated and the phonon-electron scattering increases, leading to increased resistance [15].

From Fig. 7 c and d, we can see that the patterns of changes in the electrical resistance and the gas sensitivity of the SnO_2 and that of CNTs/SnO_2 are basically the same. Within a certain range of concentration, the introduction of CNTs in the materials leads to an obvious decrease in the electrical resistance, while the gas sensitivity to alcohol increases. As the concentration of the alcohol increases, the electrical resistance of both the pure SnO_2 and the CNTs/SnO_2 composites decreases, while their gas sensitivity tends to increase and finally stabilizing at a constant.

The decrease in the electrical resistance of the materials after the introduction of CNTs can be explained by the conductivity of metallic CNTs,

which boosts the conductivity and reduced the resistance. The decrease in the electrical resistance of the materials with the increase in the concentration of the alcohol gas can be explained by the desorption of some oxygen particles physically adsorbed to the SnO_2 at the optimum working voltage. Therefore, when the alcohol CH_3CH_2OH is added, as a reducing gas, it will react with the oxygen adsorbed to the surface of SnO_2 to release electrons to surface of the materials, thereby improves their surface conductivity and reduces their resistance with increased charge carrier density. As the concentration of the alcohol gas increases further, an increasing amount of oxygen from the surface of the SnO_2 is reduced, the electrical resistance continues to weak; and when the oxygen on the surface of SnO_2 is finally exhausted, the electrical resistance accordingly stabilizes at a constant value.

We can see that the gas sensitivity of the SnO_2 materials to alcohol increases with the introduction of CNTs (Fig.7d). From the analyses above, the SnO_2 in the CNTs/SnO_2 nanocomposites is evenly distributed to form a layer of parcel on the outer wall of CNTs. The CNTs have larger specific surface area and the pretreatment process will create open-ended carbon nanotubes as well as many nanochannels. Lots of defects on the outer walls of CNTs also lead to an increased adsorption. All these factors help increase the contact between the SnO_2 nano-particles, and the alcohol, therefore lead to increased gas sensitivity readings of the materials. When the intensity of the alcohol increases within a certain range, the gas sensitivity of the materials will rise accordingly. This can be explained by the surface of the gas sensitive materials increasingly covered by the reducing gas which it has adsorbed, and the increase in the coverage accelerates, too, as the intensity of the gas increases.

In addition, the size of the SnO_2 grains is a key factor to their gas sensitivity [16]. The SnO_2 nucleation and growth of the grains on the walls of CNTs result in the formation of core-shell structure nanowires, preventing SnO_2 agglomeration. The smaller size of the SnO_2 grains leads to significantly increased specific surface area and higher gas sensitivity.

4. Conclusions

The uniformly shaped CNTs/SnO_2 core-shell structure nanowires were successful synthesized by using the solution coprecipitation method. SnO_2 nanoparticles with a diameter of 6~10 nm was evenly distributed on the outer walls of CNTs. The CNTs can prevent the agglomeration of the SnO_2 and generate smaller grains of SnO_2. The optimal working voltage of CNTs/SnO_2 composites in gas sensitivity tests is lower compared with that of pure SnO_2, therefore CNTs/SnO_2 composite materials work better than pure SnO_2 in gas sensitivity tests at lower temperatures.

The introduction of CNTs not only leads to the creation of a large amount of nanochannels that increase the contact between SnO_2 and the alcohol gas atmosphere, but also prevents the agglomeration of SnO_2. Coupled with the many defects on the surface of CNTs and dangling bonds that can help adsorb alcohol, thereby increases gas sensitivity.

REFERENCES

[1]. *M. Morsy, I. S. Yahia, H. Y. Zahran, M. Ibrahim*, Low cost alcoholic breath sensor based on SnO_2 modified with CNTs and graphene, Journal of the Korean Physical Society, **vol. 73**, 2018, pp: 1437-1443.

[2]. *W. P. Sun, X. H. Rui, M. Ulaganathan, S. Madhavi, Q. Y. Yan*, Few-layered $Ni(OH)_2$ nanosheets for high-performance supercapacitors, J. Power Sources, **vol. 295**, 2015, pp: 323-328.

[3]. *A. Choudhury, J. S. Bonso, M. Wunch, K. S. Yang, J. P. Ferraris, D. J. Yang*, In-situ synthesis of vanadium pentoxide nanofibre/exfoliated graphene nanohybrid and its supercapacitor applications, J. Power Sources, **vol. 287**, 2015, pp: 283-290.

[4]. *K. Nemeth. Z, Pallai, B. Ret, P. Berki, Z. Nemeth*, Preparing SnO_2/MWCNT nanocomposite catalysts via high energy ball milling, Journal of Nanoscience and Nanotechnology, **vol. 19,** 2019, pp: 492-497.

[5]. *S. Dhall, M. Kumar, M. Bhatnagar, B. R. Mehta*. Dual gas sensing properties of graphene-Pd/SnO_2 composites for H_2 and ethanol: Role of nanoparticles-graphene interface, International Journal of Hydrogen, **vol. 43**, 2018, pp: 7921-7927.

[6]. *L. W. Hu, Z. J. Yu, Z. Q. Hu, Y. Song, F. Zhang, H. M. Zhu, S. Q. Jiao*, Facile synthesis of amorphous $Ni(OH)_2$ for high-performance supercapacitors via electrochemical assembly in a reverse micelle, Electrochim. Acta, **vol. 174**, 2015, pp: 273-281.

[7]. *J. T. Mefford, W. G. Hardin, S. Dai, K. P. Johnston, K. J. Stevenson*, Anion charge storage through oxygen intercalation in $LaMnO_3$ perovskite pseudocapacitor electrodes, Nat. Mater. **vol. 13**, no. 7, 2014, pp: 726-732.

[8]. *H. T. Cui, J. Y. Xue, M. M. Wang*, Synthesis of high electrochemical performance $Ni(OH)_2$ nanosheets through a solvent-free reaction for application in supercapacitor, Adv. Powder Technol. **vol. 26**, 2015, pp: 434-438.

[9]. *Z. N. Yu, D. Binh, A. Danielle, J. Y. Thomas*, Energy storage: highly ordered MnO_2 nanopillars for enhanced supercapacitor performance, Adv. Mater. **vol. 25**, 2013, pp: 3302-3306.

[10]. *C. X. Hao, F. S. Wen, J. Y. Xiang, L. M. Wang, H. Hou, Z. B. Su, W. T. Hu, Z. Y. Liu*, Controlled incorporation of $Ni(OH)_2$ nanoplates into flowerlike MoS2 nanosheets for flexible all-solid-state supercapacitors, Adv. Funct. Mater. **vol. 24**, 2014, pp: 6700-6707.

[11]. *V. M. Arakelyan, M. S. Aleksanyan, R. V. Hovhannisyan, G. E. Shahnazaryan, V. M. Aroutiounian, K. Hernadi, Z. Nemeth, L. Forro*, Gas sensors made of multiwall carbon nanotubes modified by tin dioxide, Journal of Contemporary Physics, **vol. 48**, 2013, pp: 176-183.

[12]. *N. L. W. Septiani. V. K.Yusuf, B. Yuliarto et al.*. Hybrid nanoarchitecturing of hierarchical zinc oxide wool-ball-like nanostructures with multi-walled carbon nanotubes for achieving sensitive and selective detection of sulfur dioxide, Sensors and Actuators B-Chemical, **vol. 261**, 2018, pp: 241-251.

[13]. *S. Majumdar, A. Nandi, H. Saha*, Synergistic effects of dual-metal catalysts for selective butane detection by SnO_2, graphene nanocomposite sensor, IEEE Sensors Journal, **vol. 18**, 2018, pp: 6517-6526.

[14]. *N. D. Hoa, S. A. EI-Safty,* Synthesis of mesoporous NiO nanosheets for the detection of toxic NO2 gas, Chem. Eur J**. vol. 17**, 2011, pp: 12896-12901.

[15]. *H. Y. Zhang, Y. P. Ye, Z. H. Li, Y. M. Chen, P. Deng, Y. Y. Li,* Synthesis of Fe_2O_3eNi $(OH)_2$/ grapheme nanocomposite by one-step hydrothermal method for high-performance super capacitor, J. Mater. Sci. **vol. 51**, 2015, pp: 2877-2885.

[16]. *A. Al Enizi, M. Naushad.* Synthesis and characterization of highly selective and sensitive Sn/SnO_2/Ndoped carbon nanocomposite (Sn/SnO_2@NGC) for sensing toxic NH_3 gas, Chemical Engineering Journal, **vol. 345**, 2018, pp: 58-66.